Study of Cross Flow Air-Cooling Process via Water-Cooled Wing-Shaped Tubes in Staggered Arrangement at Different Angles of Attack, Part 2: Heat Transfer Characteristics and Thermal Performance Criteria

Sayed Ahmed E. Sayed Ahmed, Emad Z. Ibrahiem, Osama M. Mesalhy, and Mohamed A. Abdelatief

Abstract—An experimental and numerical study has been conducted to clarify heat transfer characteristics and effectiveness of a cross-flow heat exchanger employing staggered wing-shaped tubes at different angels of attack. The water-side Re_w and the air-side Re_a were at 5×10^2 and at from 1.8×10^3 to 9.7×10^3, respectively. The tubes arrangements were employed with various angles of attack $\theta_{1,2,3}$ from $0°$ to $330°$ at the considered Re_a range. Correlation of Nu, St, as well as the heat transfer per unit pumping power (ε) in terms of Re_a, design parameters for the studied bundle were presented. The temperature fields around the staggered wing-shaped tubes bundle were predicted by using commercial CFD FLUENT 6.3.26 software package. Results indicated that the heat transfer was increased by increasing the angle of attack from $0°$ to $45°$, while the opposite was true for angles of attack from $135°$ to $180°$. The best thermal performance and hence η of studied bundle was occurred at the lowest Re_a and/or zero angle of attack. Comparisons between the experimental and numerical results of the present study and those, previously, obtained for similar available studies showed good agreements.

Keywords—Wing-shaped tubes, Cross-flow cooling, Staggered arrangement, and CFD.

I. INTRODUCTION

HEAT exchangers have been playing a vital role in energy applications for a long time. Economical and environmental issues progressively place the needs for compactness and performance improvement of such systems. In this regard, tubes of various shapes and arrangements have been studied experimentally and numerically.

Zukauskas and Ulinskas [1] suggested correlations for heat transfer and pressure drop for in-line and staggered banks of

Sayed Ahmed E. Sayed Ahmed is Prof. Dr. at the Mechanical Power Engineering Department, Faculty of engineering, Zagazig University, Egypt, (phone: +201066325010, e-mail: sahmeds@zu.edu.eg).

Emad Z. Ibrahiem Asst. Prof. at the Mechanical Power Engineering Department, Faculty of engineering, Zagazig University, Egypt, (phone: +201226835589, e-mail: emadz20022000@yahoo.com).

Osama M. Mesalhy Dr. in Mechanical Power Engineering Department, Faculty of engineering, Zagazig University, Egypt, (phone: +201007287135, e-mail: mesalhy_osa@yahoo.com).

Mohamed A. Abdelatief eng. in Mechanical Power Engineering Department, Faculty of engineering, Zagazig University, Egypt, (phone: +201272602004, e-mail: eng_aboatia@yahoo.com).

circular tubes. Their study covered the range of $1 \leq Re_a \leq 2 \times 10^6$, and $0.7 \leq Pr \leq 500$, as well as a wide range of relative transverse and longitudinal pitches. They suggested an efficiency factor for the evaluation of heat transfer surfaces efficiency in further improvement of heat exchangers constructions. Fluid flow and heat transfer characteristics in semi-circular tube placed in cross flow, for a wide range of Re_a, have been numerically and experimentally investigated by Nada et al. [2]. They mentioned that the semi-circular tube has higher Nu_a than that of the circular one. Comparisons of circular and elliptical tubes, as the essential elements of heat exchangers, have been reported in several studies, for example, Brauer [3] reported 18 % of relative reduction in the pressure drop for elliptical tubes compared to circular ones. Horvat et al. [4] studied the transient heat transfer and fluid flow for circular, elliptical, and wing-shaped tubes with the same cross sections. Comparing the three types of tubes, they reported that the values of the average Stanton number St_a were lower for the ellipsoidal and the wing-shaped tubes than those for the cylindrical ones.

The effects of cylinders spacing and angles of attack on heat transfer for elliptical tubes in tandem arrangement were investigated by Nishiyama et al. [5]. They found that the angle of attack, as well as, the cylinders spacing influenced the local heat transfer. They concluded that the cylinders spacing and the angles of attack should be arranged as small as possible to minimize the drag and to achieve higher heat transfer rate and compactness of the system. Harris and Goldschmidt [6] investigated the effects of the variation of the tube axis ratios and angles of attack on overall heat transfer for Re_a ranging from 7.4×10^3 to 7.4×10^4. Both Re_a and Nu_a were based on the length of the major axis. They concluded that an axis ratio of 0.30 or less must be achieved to realize any appreciable change in the heat transfer coefficient (e.g. greater than 10%) over the circular tube. Ibrahim and Gomma [7] have performed experimental and numerical studies of the turbulent flow over bundle of elliptical tubes. Their investigation covered a range of Re_a from 5.6×10^3 to 40×10^3 with four axis ratios considered (0.25, 0.33, 0.5 and 1) and the flow angles of attack were varied from $0°$ to $l50°$. Their results showed that the thermal performance obtained under a fixed pumping

World Academy of Science, Engineering and Technology
International Journal of Aerospace and Mechanical Engineering
Vol:7, No:6, 2013

power was the best at $0°$ and the worst at $90°$ flow angles of attack. Ibrahim et al. [8] conducted an experimental investigation of the performance of a bundle of semi-circular tubes. Re_a was ranged from 2×10^4 to 16.5×10^4, the angles of attack were varied from $0°$ to $270°$ and the relative longitudinal pitch S_L/d was at 1.35 and 2.69, while the relative transverse pitch was kept at $S_T/d=1.35$. They concluded that the highest and the lowest values of Nu_a and effectiveness, for all values of S_L/d, were occurred at $270°$ and $0°$ angle of attack, respectively.

An experimental study of air cooling and dehumidification process around a bank of in-line elliptical tubes of cross flow heat exchanger was conducted by Ibrahiem et al. [9]. They concluded that; (a): the Colburn j-factor increases with the angle of attack α for constant relative transverse pitch for the given range of relative longitudinal pitch, (b): the effectiveness (ε) of the wet surfaces of the tested bundle increases with α. Forced convection cross-flow heat transfer of hot air over an array of cold water-carrying elliptical tubes has been, experimentally, studied for airside and waterside by Khan et al. [10]. The results showed that the heat transfer rate increased with the increase of both water and air flows. The forced convective heat transfer characteristics for incompressible fluids past a bundle of circular cylinders have been, numerically, investigated by Mangadoddy et al. [11]. Their results showed that the values of Nu_a obtained for the constant heat flux conditions were higher than those for isothermal conditions. An experimental investigation has been conducted by Ibrahim and Moawed [12] to clarify heat transfer characteristics and entropy generation for individual elliptical tubes with longitudinal fins. The investigated geometrical parameters included the placement of the fins at the frontal, the rear and both frontal and rear portions of the tubes. The results indicated that the use of fins affected the results of heat transfer coefficient, friction factor and irreversibility ratio. Sayed Ahmed et al. [13], experimentally and numerically, studied the flow and heat transfer characteristics of a cross flow heat exchanger employing staggered wing-shaped tubes with zero angle of attack. Hot air was forced to flow over the external surfaces of the tubes and exchanged heat with the cold water flowing inside. The results indicated that, the bundle of wing-shaped tubes has better performance over other bundles for similar parameters and conditions.

It can be noticed from the above discussion, to the author's knowledge, that the available data on forced convection for wing-shaped tubes are not enough. Therefore, the aim of the present study was to investigate the average heat transfer characteristics for wing-shaped tubes bundle in cross-flow with various angles of attack. To achieve these goals, experimental and numerical studies have been conducted. The tubes arrangements were employed with various angles of attack $\theta_{1,2,3}$ from $0°$ to $330°$ at the considered Re_a range.

II. EXPERIMENTAL DETAILS AND DATA COLLECTION

The experiments were conducted in an open-suction-type wind tunnel of 2780mm length, as shown in Fig. 1. The tunnel is capable of producing an air velocity up to 7.3m/s. Plexiglas test section of $(305 \times 305)mm^2$, and 780mm long is mounted in the middle of the wind tunnel. The cross-sectional dimensions of wing-shaped tube, drawn from 1mm thick, 22.5mm outer diameter circular copper tube with 305 mm long, is shown in Fig. 2 (a). The tested tube bundle, shown in Fig. 2 (b), consists of 22 wing-shaped tubes distributed through three successive rows in addition to four half dummy ones. The tubes of the bundle could be fixed in the test section with a special mechanism having the capability of changing the flow angle of attack $(\theta_{1,2,3})$, while the longitudinal (S_L) and transverse (S_T) tube-pitches of 37mm were kept constant. The flow angle of attack, as illustrated in Fig. 3, could be adjusted by turning the tube, clockwise, around a vertical axis at the center of a flat surface using a protractor mechanism. When θ was kept constant for all tubes of the same row it denoted as the row flow angle of attack (θi), where i = 1, 2 and/or 3.

Different tubes arrangements for various $\theta_{1,2,3}$ were considered. $\theta_{1,2,3}$ was changed from $0°$ to $315°$ ($0°$, $45°$, $135°$, $180°$, $225°$, and $315°$) experimentally and from $0°$ to $330°$ ($0°$ [Fig. 2 (b)], $30°$, $45°$, $135°$, $150°$, $180°$, $210°$, $225°$, $315°$, and $330°$) numerically at the considered Re_a range. Air was heated via 4kW electrical heater installed in the entrance of the wind tunnel. Air at $56.5 \pm 1.5°C$ dry bulb and $26 \pm 1.5°C$ wet bulb temperature entered the test section and passed over the tubes bundle. A 134A refrigeration system was employed for keeping the, flowing inside tubes, water at $10.8 \pm 1.5°C$.

A. Measuring Techniques

T-type thermocouples were used to measure the temperatures. Water flow inlet, T_{wi} and exit, T_{we} temperatures, were measured by means of a single point measurement. Air flow inlet, T_{ai} and exit, T_{ae} average temperatures, were measured via 8 thermocouples arranged uniformly on two grids at the entrance and the exit of the test section. The wet bulb temperatures at the inlet and the exit were measured by using alcohol thermometer with wet wick surrounded bulb. The surface temperatures of the tubes, T_s were measured by attaching 2 thermocouple probes on the outer surface of each tube of the tested bundle. The average temperature of every tube was taking to be as the average of the two probes attached to its surface. A hand-held digital thermometer with an uncertainty of $\pm 0.2°C$ with $\pm 0.1°C$ sensitivity was used to record the temperatures. The airflow pressure drop (ΔP_a) caused by the studied bundle was measured via an electrical micro-manometer of $\pm 0.1mm$ H_2O accuracy of full scale, (manufactured by Furness controls company, model FC 001, and serial number (FN 2561), which was connected to 4 pressure taps as depicted in Fig. 4.

Sufficient time, from about 120 to 160min., was allowed for getting the desired air temperature stabilization. Experimental data was involved the temperature measurements of the tubes surfaces, air inlet and exit and water inlet and exit as well as the water mass flow rates corresponding to four predetermined values of mean air velocity in the wind tunnel.

Four different cold-water mass flow rates (m_w) of 0.205, 0.26, 0.35 and 0.43kg/s were considered. The water flow rates

World Academy of Science, Engineering and Technology
International Journal of Aerospace and Mechanical Engineering
Vol:7, No:6, 2013

were measured, at the beginning of each test run, using bucket stopwatch method. The mean velocity (V_{ai}) of the air flow was varied from 1.33 to 7m/s, yielding Re_a from 1.8×10^3 to 9.7×10^3 while $Re_w = 5 \times 10^2$. The air velocities for subsequent experiments were measured at a single point around the entrance-center of the test section with a 3mm Pitot static tube using the same electrical micro-manometer as used in the pressure drop measurement. All of the experiments were conducted at the same inlet conditions with Re_a and Re_w, based on the tube equivalent diameter D_{eq}.

DRAWING LEGEND	
NO.	Description
1	Electrical Heaters
2	Honey Comp
3	Pitot-Static tube
4	Pressure taps
5	Test section
6	Gate
7	Centrifugal Fan
8	Electrical motor
9	Water control valves
10	Water pump
11	Electrical micro-manometer
R-134a Refrigeration System	
12	Water tank
13	Evaporator
14	1.5 hp Compressor
15	Expansion valve
16	Condenser

- - - - Refrigeration Circuit

───── Water circuit

Fig. 1 Schematic Drawing of The Experimental Setup

(a)

(b)
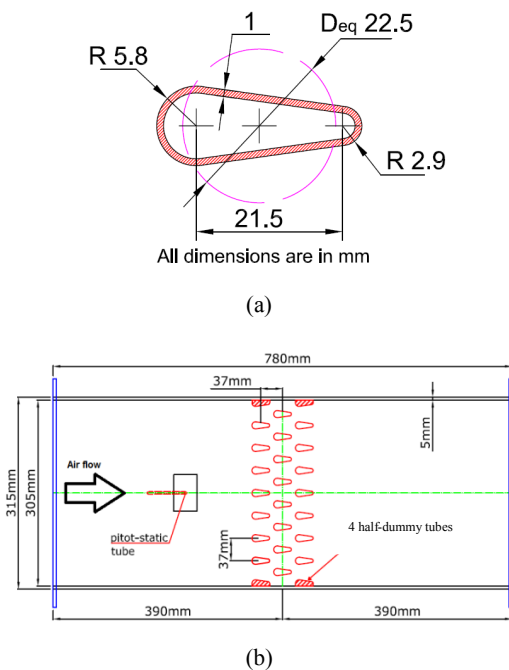
Fig. 2 (a) Wing- Shaped Tube Cross Sectional Dimensions (b) Schematic Plane of the Test Section, $\theta_{1,2,3} = 0°$, (Case 1)

B. Data Reduction

Steady state flow conditions were achieved during the experiments. The fluid properties, for both air and water, were determined from tables given by Cengel [14]. If not mentioned otherwise, all the thermo-physical properties for air were evaluated at the air film temperature. Considering a linear variation of temperature between the outer surface of the tubes and the approaching air, the air film temperature was deduced as follows: $\left(T_{af} = \dfrac{T_{ai} + T_s}{2} \right)$, while for water at bulk temperature, T_{wb}.
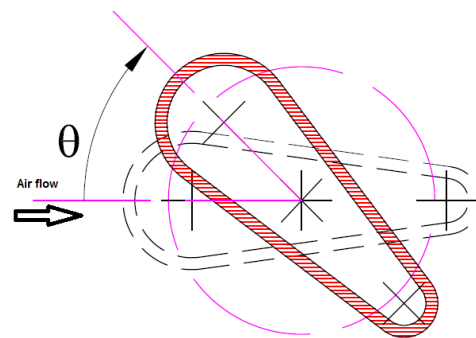

Fig. 3 The adjusting of flow attack angle

World Academy of Science, Engineering and Technology
International Journal of Aerospace and Mechanical Engineering
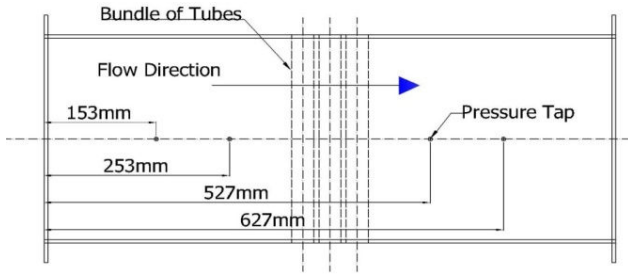Vol:7, No:6, 2013

Fig. 4 The locations of the pressure taps

1. Fluid Flow Considerations

Mean inlet air velocity was calculated from the measured data by the standard Pitot tube through the following relationship:

$$V_{ai} = \sqrt{2g\left(\rho_w / \rho_{af}\right)\Delta h_{dyn}}, \quad (m/s) \tag{1}$$

where, Δh_{dyn} is the head difference between the total and static pressure heads through Pitot tube, m H_2O, while ρ_w and $\rho_{a,f}$ are the average densities for water and air respectively, kg/m^3.

The pressure drop coefficient, P_{dc}, as defined below in (2), represents the ratio of the total pressure drop of the moving air over the tube bundle to its dynamic pressure

$$P_{dc} = \frac{2\Delta p_a}{\rho_{af} V_{ai}^2} \tag{2}$$

where, the pressure drop through the tube bundle, Δp_a was measured by the electrical micro-manometer via pressure taps, and ρ_{af} is the air film density.

2. Heat Transfer Rate Considerations

By applying heat balance on the test section control volume, the overall heat transfer rate from the air or to the cooling water can be expressed as,

$$Q = Q_{overall} = Q_{convection} + Q_{radiation} + Q_{condensation} \tag{3}$$

The water-side and air-side heat transfer rates were estimated as:

$$Q_w = m_w c_{pw}(T_{we} - T_{wi}) = m_w c_{pw} \Delta T_w \tag{4}$$

$$Q_a = m_a c_{p_{af}}(T_{ai} - T_{ae}) = m_a c_{p_{af}} \Delta T_a \tag{5}$$

where, m_w and m_a (kg/s) are the mass flow rates for water and air, respectively. T_{wi}, T_{we}, T_{ai}, T_{ae} are the water and air inlet and exit temperatures, respectively.

The heat transfer rates at waterside were compared with those of the airside. Thus in the analysis, the overall heat transfer rate, Q, was set to the arithmetic average of the airside and waterside heat rates in the following form,

$$Q = \frac{Q_a + Q_w}{2} \tag{6}$$

The influence of radiation heat transfer between the tubes surfaces and the surrounding environment inside the test section was ignored (i.e. $Q_{radiation} \approx 0$).

During the tests, the temperatures of the tubes surfaces were kept higher than the dew point temperature of the flowing air, so the condensation of the flowing air moisture was avoided (i.e. $Q_{condensation} \approx 0$). Thus, heat transfer between air and water was occurred, mainly, due to the forced convection mechanism. Therefore, by setting the overall heat transfer rate, $Q_{overall}$, to the average heat transfer rates at waterside and airside, (3) could be rewritten as:

$$Q = Q_{overall} \approx Q_{convection} = h_a A_{so} \Delta T_{ln} \tag{7}$$

where, A_{so}, is the total outer surface area for the tubes and, ΔT_{ln} is the logarithmic mean temperature difference.

$$\Delta T_{ln} = \frac{T_{ai} - T_{ae}}{\ln\left(\frac{T_{ai} - T_s}{T_{ae} - T_s}\right)} \tag{8}$$

The air-side average heat transfer coefficient was determined as:

$$h_a = \frac{Q}{A_{so} \Delta T_{ln}} \tag{9}$$

The Reynolds number, Re_a was given by:

$$Re_a = \frac{\rho_{af} V_{ai} D_{eq}}{\mu_{af}} \tag{10}$$

The Nusselt number was attributed as:

$$Nu_a = \frac{h_a D_{eq}}{k_{af}} \tag{11}$$

where, D_{eq} is the outer equivalent diameter of the tube and k_{af} is the air thermal conductivity, W/m.K. The experimental error analysis indicated the implication of error of the measured parameters on the uncertainty of the results.

World Academy of Science, Engineering and Technology
International Journal of Aerospace and Mechanical Engineering
Vol:7, No:6, 2013

III. NUMERICAL INVESTIGATION

A. Problem Description and Boundary Conditions

Since, the tube length is much greater than its equivalent diameter, the flow across the tube bundle is considered two-dimensional. The geometry of the numerical model includes entrance section, tube bundle section, and exit section beside the boundary conditions, are shown in Fig. 5. The numerical solution is carried out by solving the governing equations of mass, momentum and energy under the following assumptions; the flow is incompressible, steady and turbulent, fluid properties are constant, the effect of buoyancy force and radiation are neglected, Fluent [15]:

$$\frac{\partial}{\partial x_i}(\rho \ V_i) = 0.0 \quad (12)$$

$$\frac{\partial}{\partial x_j}(\rho V_i V_j) = -\frac{\partial p}{\partial x_i} + \frac{\partial \tau_{ij}}{\partial x_j} \quad (13)$$

$$\frac{\partial}{\partial x_i}[V_i(\rho E + p)] = \frac{\partial}{\partial x_i}\left(k \frac{\partial T}{\partial x_i}\right) \quad (14)$$

where, i: is a tensor indicating 1 and 2, τ_{ij} is the viscous stress tensor, and k is the fluid effective thermal conductivity.

Commercial CFD software FLUENT 6.3.26 was used to solve the governing equations. RNG $\kappa-\varepsilon$ turbulent model is utilized to solve the complicated turbulent thermal flow field with Enhanced Wall Function approach in the near-wall regions to fit the wall boundary conditions, Fluent [15].
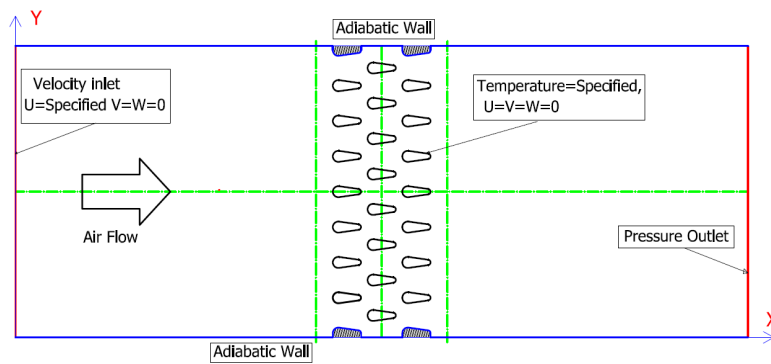

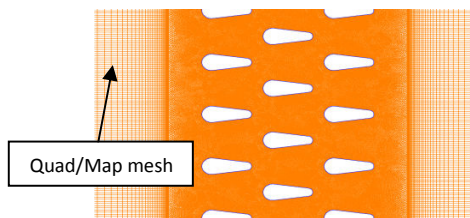Fig. 5 Boundary conditions for the numerical domain

B. Mesh Generation and Discretization

The geometry and mesh of the computational model that described in the previous section were generated separately using GAMBIT 2.4.6. Quad/Map, Tri/Pave and boundary layer meshing scheme was used in the present study with refining the mesh near walls and beside sharp edges. Figs. 6 and 7 show the configuration of the computational domain mesh. A finite volume discretization method using second order upwind schema for momentum, turbulent kinetic energy, and turbulent dissipation rate was applied, besides using simple-based solution algorithm of the velocity–pressure coupling with a segregated solver. The solution was considered converged when the scaled residual of the energy equation reaches 10^{-7} and the scaled residuals of other equations reach 10^{-4}.
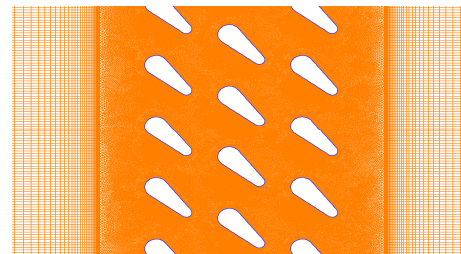
(b) $\theta_{1,2,3} = 45°$

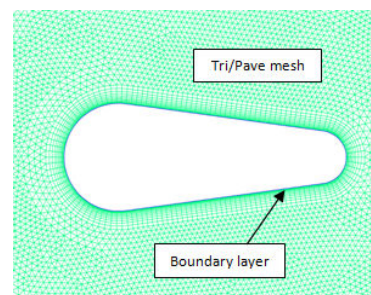Fig. 6 Mesh configurations for the domain of the tubes bundle

Fig. 7 Mesh details around the wing-shaped tube

(a) $\theta_{1,2,3} = 0°$

World Academy of Science, Engineering and Technology
International Journal of Aerospace and Mechanical Engineering
Vol:7, No:6, 2013

IV. RESULTS AND DISCUSSION

A. Heat Transfer Characteristics Over the Bundle of Wing-Shaped Tubes

Temperature contours for the air flowing across the tubes are depicted in Fig. 8. For, the comparatively, low Re_a it is noticed that the thermal boundary layer is thicker than that for the higher Re_a. This is attributed to the separation of the flow over the tubes surfaces leading to the increase of h_a, and Nu_a with Re_a. It is seen from the figure, also, that the heat transfer rate for arrangement with $\theta_{1,2,3} = 45^{\circ}$ is higher than that with $\theta_{1,2,3} = 0^{\circ}$.

$$Re_a = 1.8 \times 10^3 \quad Re_a = 9.7 \times 10^3$$
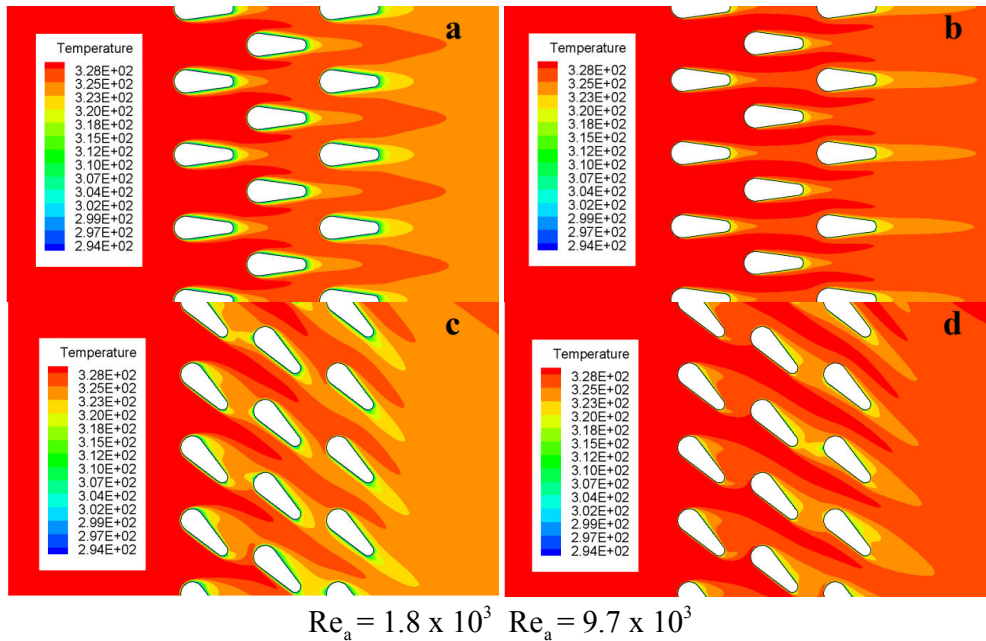
Fig. 8 Temperature contours for different arrangements, [(a) & (b) for $\theta_{1,2,3} = 0^{\circ}$], [(c) & (d) for $\theta_{1,2,3} = 45^{\circ}$]

1. Effect of Reynolds Number Rea on Heat Transfer

The numerical results of the present study were validated with the corresponding experimental ones. Fig. 9 shows the experimental and numerical validation of Nu_a with Re_a for the first case. Results show that the thermal resistance of the air and hence the Nu_a at the lower Re_a are higher than those obtained at the higher Re_a. Also, the figure shows that both numerical and experimental results have, nearly, the same values and the same trend. The average estimated error between the numerical and experimental results is $\approx 6\%$. In other words, increasing angle of attack agitates the boundary layer, further increasing angle of attack leads to progressively lesser boundary layer alteration. It is clear, also, from the figure that Nu_a increases with Re_a and/or angle of attack. This is may be attributed to the increase of turbulent intensity, leading to the amplification of the convective heat transfer. The highest and lowest values of Nu_a are obtained at $\theta_{1,2,3} = 45^{\circ}$, 135° and at $\theta_{1,2,3} = 0^{\circ}$, 180°, respectively.

(a) Numerical

World Academy of Science, Engineering and Technology
International Journal of Aerospace and Mechanical Engineering
Vol:7, No:6, 2013

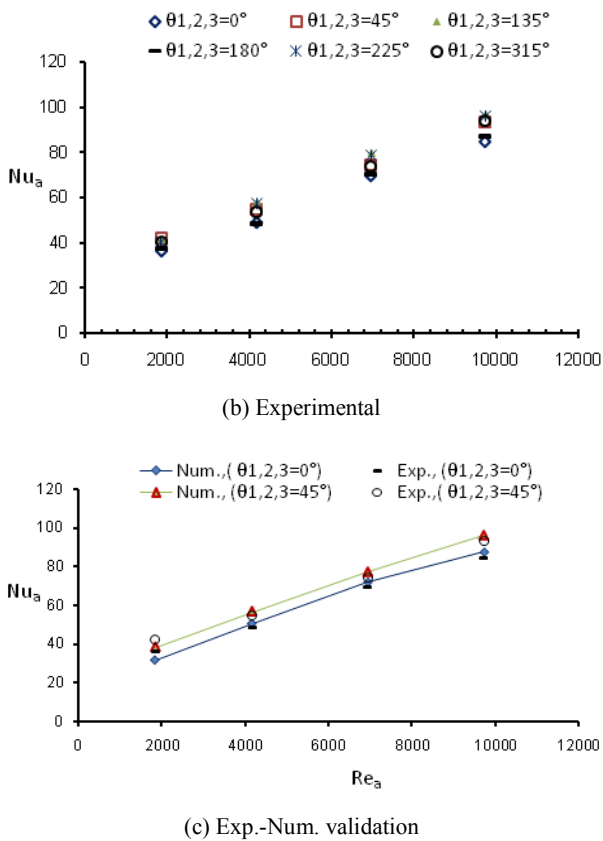(b) Experimental

(c) Exp.-Num. validation
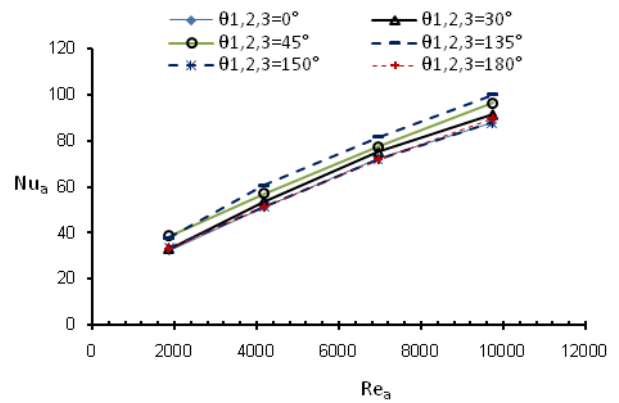
Fig. 9 Validation of Nu_a versus Re_a for different flow angles of attack

Fig. 10 shows the validation of Nu_a versus angle of attack ($\theta_{1,2,3}$) at different Re_a. It is seen from the figure that, at a certain Re_a, the highest values of Nu_a are occurred at $\theta_{1,2,3} = 45°, 135°, 225°, 315°$, this can be attributed to the high level of turbulence intensity and the induced secondary flows. On the other hand the lowest values are occurred at $\theta_{1,2,3} = 0°, 180°$.

Fig. 10 Validation of Nu_a versus angle of attack ($\theta_{1,2,3}$) at different Re_a
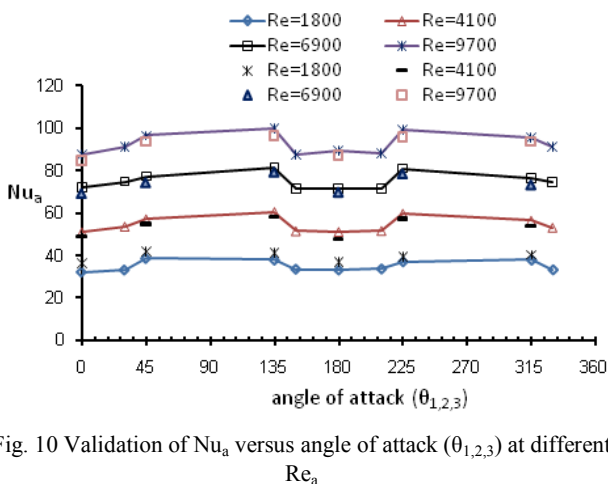
Fig. 11 presents the experimental and numerical validation of St_a as a function of Re_a for the angles of attack $\theta_{1,2,3} = 0°, 30°, 45°, 135°, 150°,$ and $180°$ numerically and $\theta_{1,2,3} = 0°, 45°,$

$135°, 180°, 225°, 315°$, experimentally. The results show that, the St_a always decreases with Re_a increasing. The St_a first rapidly decreases with increasing Re_a and then gradually decreases with Re_a. This could be attributed to the fact that the rate of Nu_a increasing is lower than for Re_a increasing. The highest value of St_a is occurred at $\theta_{1,2,3} = 45°$, while the lowest value of St_a is occurred at $0°$. The St_a distributions shows a good agreement between the numerical and the experimental values obtained for the whole range of Re_a as shown in Fig. 11 (c). The agreement demonstrates the correctness of the selected numerical approach.
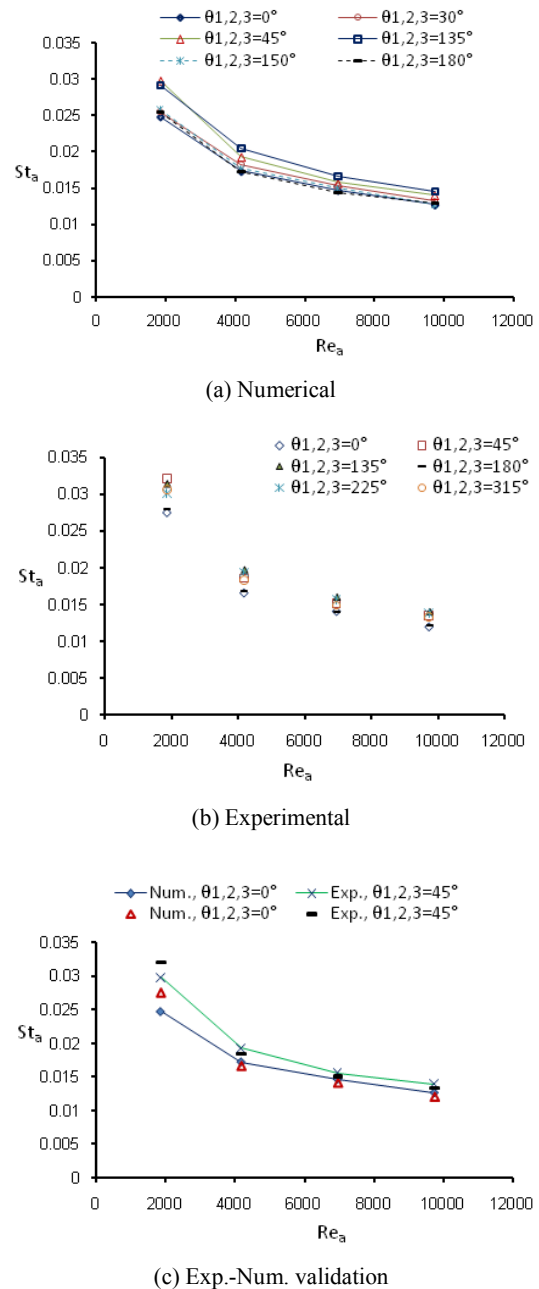

(a) Numerical

(b) Experimental

(c) Exp.-Num. validation

Fig. 11 Experimental and numerical validation of St_a versus Re_a at different flow angles of attack

World Academy of Science, Engineering and Technology
International Journal of Aerospace and Mechanical Engineering
Vol:7, No:6, 2013

Fig. 12 shows the numerical and experimental validation of St_a versus various $\theta_{1,2,3}$ at different Re_a. It is seen from the figure that at a certain Re_a, the highest and lowest values of St_a are occurred at $\theta_{1,2,3} = 45°, 135°, 225°, 315°$ and at $\theta_{1,2,3} = 0°$, $180°$, respectively. At high Re_a the variation of St_a are gradually smooth for smaller angles of attack, and at low Re_a the St_a is rapidly. This means that the flow velocity increases faster than the convective heat transfer from the isothermal walls to the fluid. Therefore, the average outlet air temperature $T_{a,o}$ decreases with increasing Re_a.
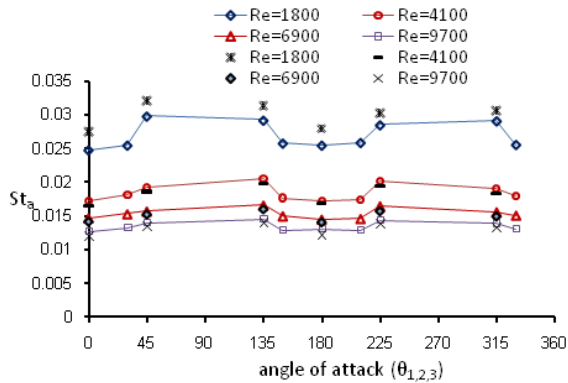
Fig. 12 Experimental and numerical validation of St_a versus angle of attack at different Re_a

Correlations for Nu_a and St_a based on the experimental results obtained for various $\theta_{1,2,3}$ and Re_a, with a maximum deviation $\approx \pm 11\%$, were predicted by (15) and (16) as follows:

$$Nu_a = a.\left(Re_a\right)^b.\left(Pr\right)^{\frac{1}{3}}.\left(1+\frac{\theta°}{\theta°_{90°}}\right)^c \quad (15)$$

$$St_a = a.\left(Re_a\right)^{b-1}.\left(Pr\right)^{-\frac{2}{3}}.\left(1+\frac{\theta°}{\theta°_{90°}}\right)^c \quad (16)$$

Table I shows all the constants for Nu_a and St_a. The excellent R^2 values confirm the statistical goodness of the fit. The obtained correlations are applicable for $1.8 \times 10^3 \leq Re_a \leq 9.7 \times 10^3$. Prandtl number of the flowing air, Pr_{af}, was, nearly, considered constant (≈ 0.706).

TABLE I
CONSTANTS AND R^2 FOR PROPOSED CORRELATION FOR NUSSELT AND STANTON NUMBERS

	a	b	c	R^2
$0° \leq \theta_{1,2,3} \leq 45°$	0.52	0.567	0.272	0.986
$135° \leq \theta_{1,2,3} \leq 180°$	1.1323	0.5631	-0.6737	0.985
$180° \leq \theta_{1,2,3} \leq 225°$	0.2334	0.5732	0.6829	0.984
$315° \leq \theta_{1,2,3} \leq 360°$	2.327	0.5741	-0.9691	0.987

B. Comparison of the Present Study Heat Transfer Results with Others from the Literature

The current proposed heat transfer correlations for the bundle of wing-shaped tubes, (15) and (16) were compared with others found in the literature. One of those was based on the experimental work for flow over circular staggered tube banks, Zukauskas [16] as referenced by Cengel, Y. A. [14] as the following

$$Nu_a = 0.35({S_T}/{S_L})^{0.2} Re_a^{0.6} Pr_{af}^{0.36} ({Pr_{af}}/{Pr_s})^{0.25} \quad (17)$$

$$(1000 \leq Re_a \leq 2 \times 10^5)$$

where, S_T and S_L are the transverse and longitudinal tube-pitches, respectively. By applying a correction factor and other parameters from the present study, the above equation could be written as follows:

$$Nu_a = 0.31 Re_a^{0.6} \quad (1000 \leq Re_a \leq 2 \times 10^5) \quad (18)$$

$$St_a = 0.44 Re_a^{-0.4} \quad (1000 \leq Re_a \leq 2 \times 10^5) \quad (19)$$

Ibrahim and Gomma [7] proposed a heat transfer correlation for elliptical tubes bundle in cross flow of air in the following form:

$$Nu_a = 0.452 Re_a^{0.537} \ Pr_{af}^{0.33} (\frac{a}{b})^{-0.079} (\sin(10+\alpha))^{0.2} \quad (20)$$

where, a and b are the minor and major axis of the elliptical tube, respectively. while, α is the flow angle of attack and Pr_{af} taken at the average T_{af}. To give the same surface area as wing shaped tube of the present study, a and b are substituted by 0.0131 and 0.0301 m, respectively. By employing the present experimental condition and using the tube D_{eq}, (20) could be reduced to:

$$Nu_a = 0.4302\left(Re_a\right)^{0.537}.\left(\sin(10+\alpha)\right)^{0.2} \quad ,(5300 \leq Re_a \leq 28000) \quad (21)$$

$$St_a = 0.61\left(Re_a\right)^{-0.463}.\left(\sin(10+\alpha)\right)^{0.2} \quad ,(5300 \leq Re_a \leq 28000) \quad (22)$$

Other empirical correlations were established as proposed in (23) and (24), for heat transfer characteristics of a cross flow heat exchanger employing staggered wing shaped tubes with zero angle of attack, Sayed Ahmed et al. [13].

World Academy of Science, Engineering and Technology
International Journal of Aerospace and Mechanical Engineering
Vol:7, No:6, 2013

$$Nu_a = 0.94 Re_a^{0.483}, \quad R^2 = 0.95 \quad (23)$$

$$St_a = 1.32 Re_a^{-0.518}, \quad R^2 = 0.96 \quad (24)$$

$$1.85 \times 10^3 \leq Re_a \leq 9.7 \times 10^3$$

The Nu_a and S_{ta} correlations with Re_a obtained from the present study were compared with other results from previous studies as shown in Figs. 13 and 14. As seen from Fig. 13 (a), the correlations from the present study have satisfactory agreement with that proposed by Sayed Ahmed et al. [13] at zero angle of attack and for the given range of Re_a. The studied bundle has increased values of Nu_a by about 24% and 76% comparing with those obtained for circular and elliptical tubes, respectively, for zero angle of attack.

Fig. 13 (b) shows that the values of Nu_a, obtained for $\theta_{1,2,3} = 45°$ of the present study are more than those for the elliptical tube bundle by about 64 %.
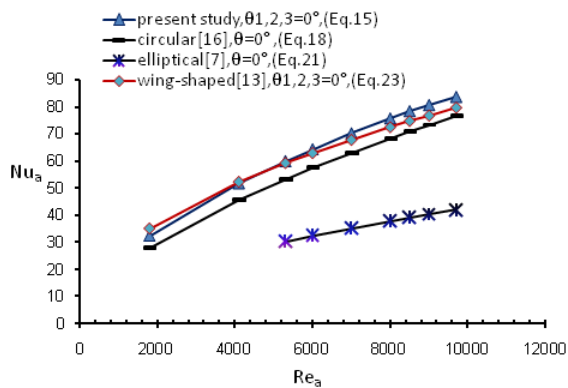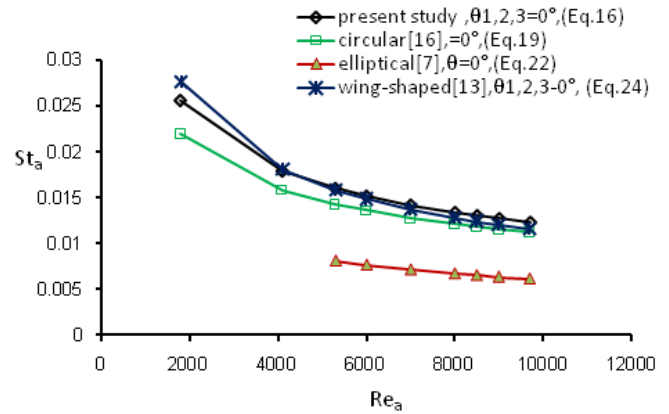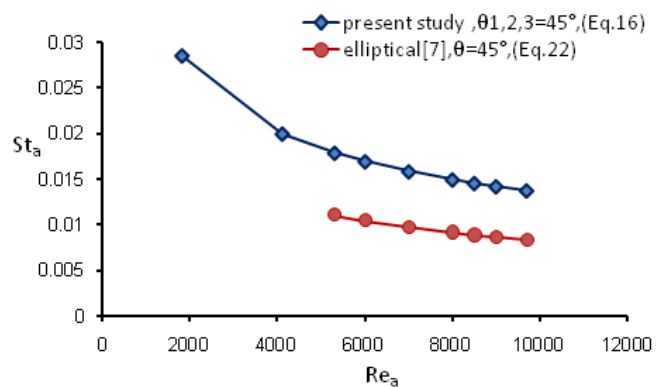

(a) For zero angle of attack
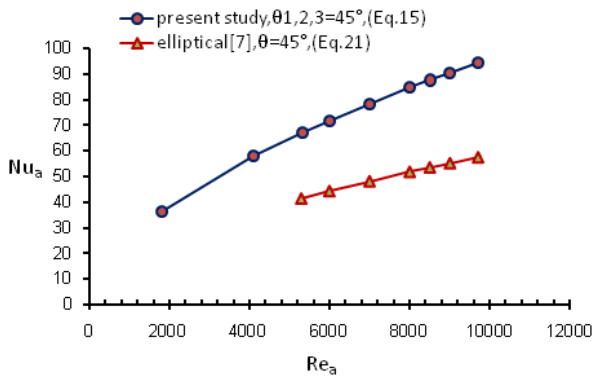
(b) For 45° angle of attack

Fig. 13 Comparison of present Nu_a vs Re_a results with previous works for different tube shapes and angles of attack

Fig. 14 shows the relationship between St_a and Re_a for the wing-shaped, circular and elliptical tubes bundles. It can be seen from the figure that the studied bundle has the highest values of St_a comparing with the others.

(a) For zero angle of attack

(b) For 45° angle of attack

Fig. 14 Comparison of present St_a vs. Re_a results with previous works of different tube shapes and angles of attack
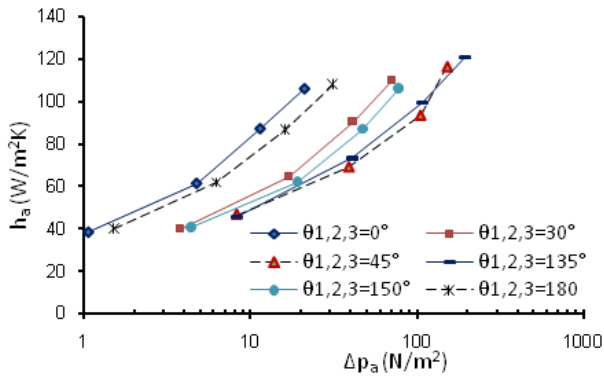
C. Thermal Performance Criteria

Three methods are presented to resort a metric that expresses the global performance of the studied bundle heat exchanger of wing-shaped tubes with the particular reference of the traditional bundle heat exchangers with circular and elliptical tubes. These methods play as the key design factors of heat exchanger whilst incorporating an economic indicator, which are:
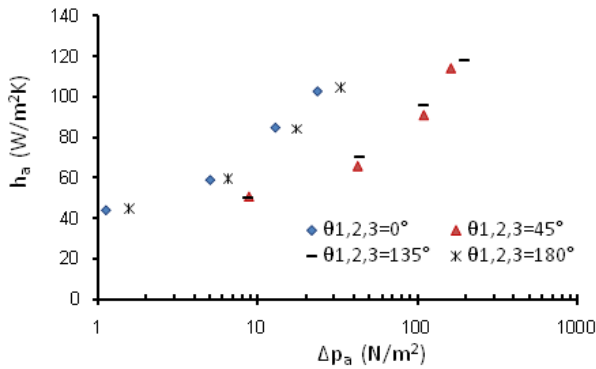
1. Direct Comparison Method

Direct comparison between the heat transfer coefficient ha and the pressure drop ΔP_a at a fixed Re_a is conducted. This criterion allows quantifying the heat transfer enhancement for different tubes bundle configurations with equivalent total pressure drops independently on the tube cross-sectional shape, Bergles et al. [17].
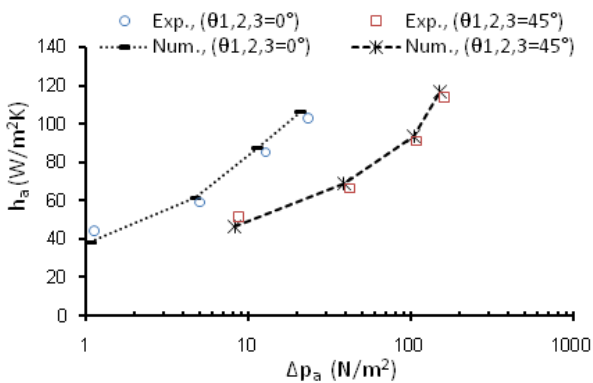
Fig. 15 shows the effect of ΔP_a on ha and their validation. The highest values of h_a were obtained for arrangement of $\theta_{1,2,3} = 0°$ while lowest ones were obtained for $\theta_{1,2,3} = 45°$, $135°$ for all values of Re_a at certain ΔP_a.

World Academy of Science, Engineering and Technology
International Journal of Aerospace and Mechanical Engineering
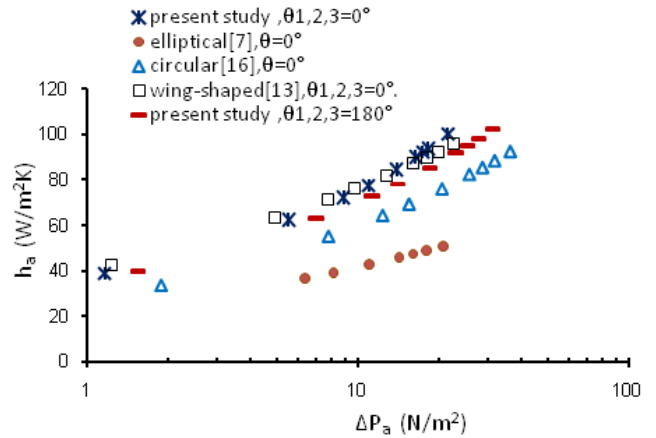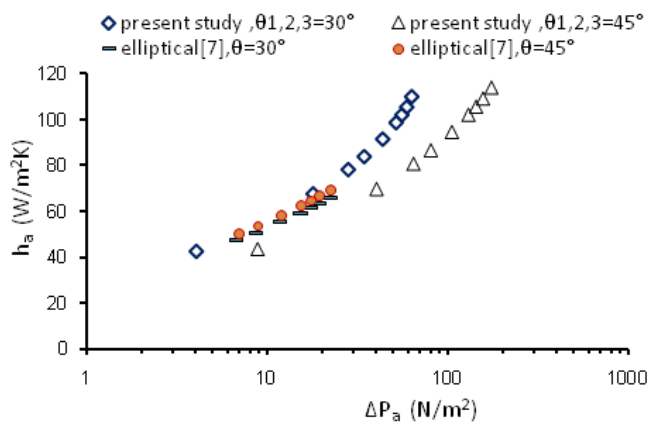Vol:7, No:6, 2013

(a) Numerical

(b) Experimental

(c) Experimental-numerical validation

Fig. 15 Experimental-numerical validation of heat transfer coefficient versus pressure drop for different flow angles of attack

(a) For $\theta_{1,2,3} = 0°$ and $180°$..

(b) For $\theta_{1,2,3} = 30°$ and $45°$

Fig. 16 Heat transfer coefficient h_a versus pressure drop ΔP_a for bundle heat exchangers with different tubes shapes

Fig. 16 shows the plot of ha versus ΔP_a for different tubes shapes. It is seen from the figure that, the agreement between the present study results and these proposed by Sayed Ahmed et al. [13] at zero angle of attack could be termed as good. Also the studied bundle has the highest values of ha at $\theta_{1,2,3} = 0°$ followed by $180°$, and $30°$, comparing with the circular and elliptical tubes bundles, at the same Re_a and pressure drop. Conversely, the elliptical tubes bundle has a higher ha than that of the studied bundle at $\theta_{1,2,3} = 45°$. The lower value of h_a has related to the bundle with elliptical tubes at zero attack angle.
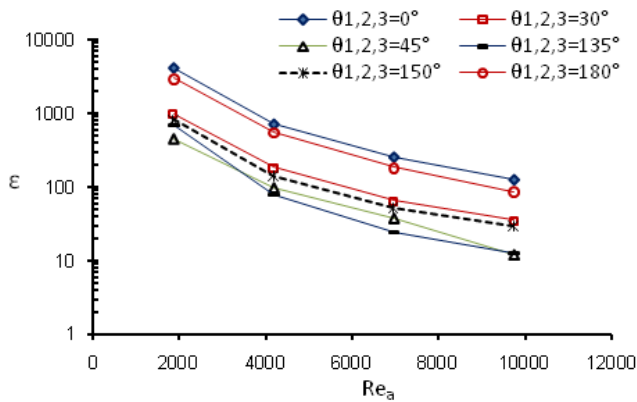
2. Effectiveness ε Method

Effectiveness (ε) represents the heat transfer per unit pumping power as stated by Gomaa et al. [18] obtained (25) for ε as follows.
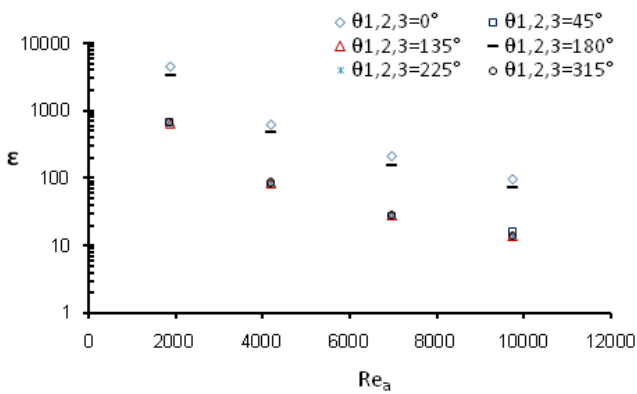
$$\varepsilon = \frac{\rho_{af} \, c_{p_f} (T_{ai} - T_{ae})}{\Delta P_a} \quad (25)$$

As seen from (25) ε presents the ratio between the amount of heat being transferred by the heat exchanger and the pumping power.

Fig. 17 shows, experimentally and numerically, the effect of Re_a on ε. It is seen from the figure that ε decreases with Re_a increasing for all arrangements. Although the heat exchanger with arrangement of $\theta_{1,2,3} = 45°$ has the highest values of Nu_a, as mentioned before, it has the lowest values of (ε). On the other hand, the wing-shaped tubes bundle with $\theta_{1,2,3} = 0°$ has the highest values of ε.

World Academy of Science, Engineering and Technology
International Journal of Aerospace and Mechanical Engineering
Vol:7, No:6, 2013

(a) Numerical

(b)Experimental

Fig. 17 Effectiveness (ε) versus different flow angles of attack

Fig. 18 shows the effect of angle of attack on the effectiveness (ε) at different Re_a and their validation. It is clear from the figure that the highest and lowest values of (ε), for all the studied arrangements, are occurred at the lowest and highest values of Re_a, respectively, while the highest and lowest values of (ε) at every Re_a are occurred at $\theta_{1,2,3} = 0°$, $180°$ and $\theta_{1,2,3} = 45°$, $225°$, respectively. Also, ε decreases from $\theta_{1,2,3}$

= $0°$ to $45°$ and $\theta_{1,2,3} = 180°$ to $225°$ while increases from $\theta_{1,2,3} = 135°$ to $180°$ and from $\theta_{1,2,3} = 315°$ to $330°$ for all considered Re_a range.
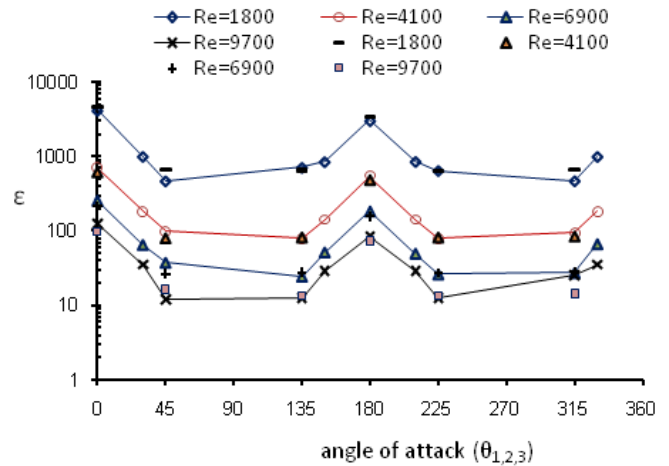

Fig. 18 Validation of effectiveness (ε) versus flow angles of attack at different Re_a

To optimize the thermo-fluid characteristics of heat exchangers, it is important to recognize, not only the enhancement of the heat transfer but also, the minimization of the pumping power usage. The effectiveness (ε) could be correlated in terms of Re_a, Pr and $\theta_{1,2,3}$ with a maximum deviation of ±12 % for a wide range of validity as presented in (26). Table II shows all the constants for (26).

$$\varepsilon = a \ (Re_a)^b \ (Pr)^{1/3} \ (1+\frac{\theta°}{\theta_{90°}})^c$$

$$1.8 \text{ x } 10^3 \le Re_a \le 9.7 \text{ x } 10^3 \tag{26}$$

TABLE II
CONSTANTS AND R^2 FOR (26)

	a	b	c	R^2
$0° \le \theta_{1,2,3} \le 45°$	413.54x10⁹	-2.421	-4.71	0.99
$135° \le \theta_{1,2,3} \le 180°$	100.64x10⁵	-2.36	8.9723	0.99
$180° \le \theta_{1,2,3} \le 225°$	2.4473x10¹⁶	-2.3595	-10.714	0.99
$315° \le \theta_{1,2,3} \le 360°$	6.0264x10⁻²	-2.4193	18.357	0.99

Ibrahim and Gomma [7] proposed a correlation of (ε) for elliptical tubes bundle in cross flow of air in the following form:

$$\varepsilon = 1.41 \ Re_a^{-2.65} \ Pr_{af}^{0.33} (\frac{a}{b})^{-1.11} (\sin(10+\alpha))^{-15.33} \tag{27}$$

By applying the present experimental condition and using the D_{eq} to define Re, (27) could be reduced to:

$$\varepsilon = 3.164 \ Re_a^{-2.65} \ (\sin(10+\alpha))^{-15.33} \tag{28}$$

Another empirical correlation (29) for staggered wing-shaped tubes bundle with zero angle of attack was established by Sayed Ahmed et al. [13].

$$\varepsilon = 1.259 \times 10^{11} Re_a^{-2.28}, \quad R^2 = 0.97$$

$$1.8 \times 10^3 \le Re_a \le 9.7 \times 10^3 \tag{29}$$

World Academy of Science, Engineering and Technology
International Journal of Aerospace and Mechanical Engineering
Vol:7, No:6, 2013

Fig. 19 shows the dependence of ε on Re_a for heat exchangers with wing-shaped, elliptical and circular tubes. It is seen from the figure that the obtained results of ε for the present study are in good agreement with these obtained by Sayed Ahmed et al. [13]. Heat exchangers with wing-shaped and elliptical tubes have, approximately, the same values of ε at 45° angle of attack.
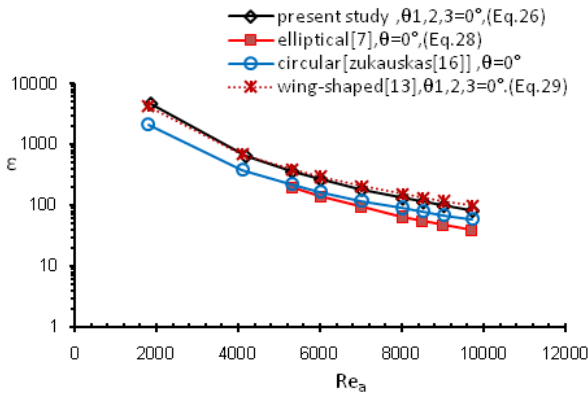
(a) $\theta_{1,2,3} = 0°$
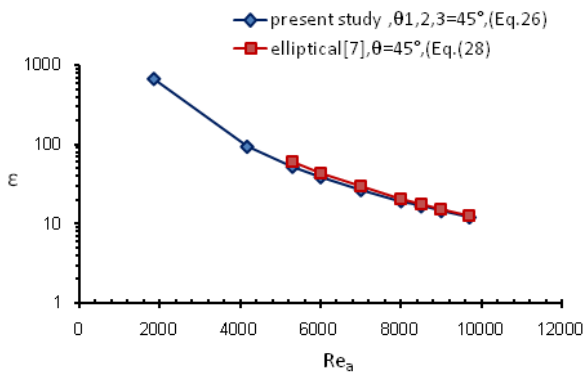
(b) $\theta_{1,2,3} = 45°$

Fig. 19 Effectiveness ε correlation for bundles with different tubes shapes

3. The Efficiency Index η Method

The efficiency index η expresses the relation between the heat transfer and the pressure drop characteristics for bundles with wing-shaped and elliptical tubes based on the relation obtained for the bundle with circular tubes. Afify et al. [19] proposed the following correlation:

$$\eta = \frac{\left(St/St_c \right)}{\left(P_{dc}/P_{dc_c} \right)} \qquad (30)$$

Fig. 20 illustrates the relationship between the efficiency index η and the Re_a for bundles with wing-shaped and elliptical tubes at different flow angles of attack. It is seen from the figure that the present study results are in good

agreement with these at zero angle of attack proposed by Sayed Ahmed et al. [13].

It is evident that the wing-shaped tubes heat exchanger with zero angle of attack has the highest values of (η) followed by the angle of attack 30° and 45°. The studied heat exchanger with zero angle of attack has the highest values of η comparing with these of elliptical ones at different flow angles of attack.
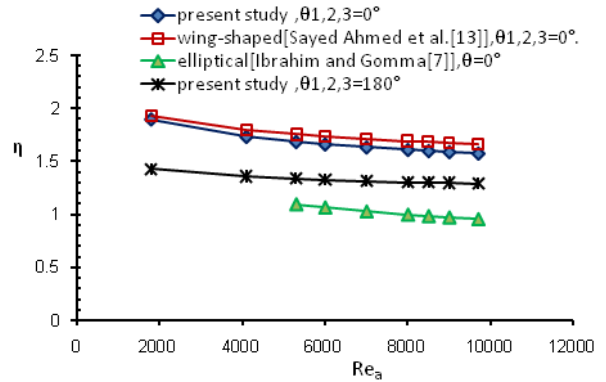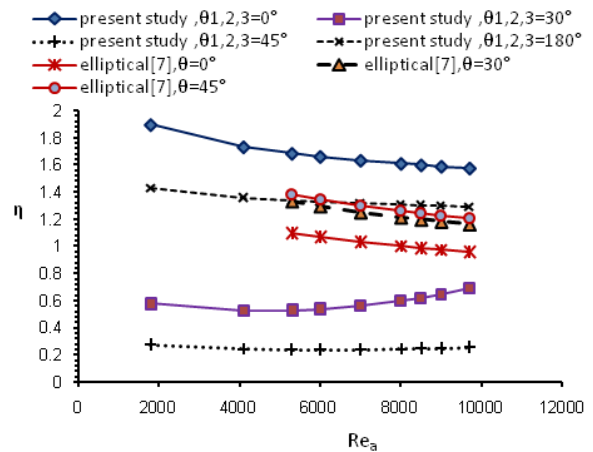
(a) For $\theta_{1,2,3} = 0°$ and 180°.

(b) For $\theta_{1,2,3} = 0°$, 30°, 45° and 180°.

Fig. 20 Efficiency index η versus Re_a for bundles of wing-shaped and elliptical tubes with different flow angles of attack

The above mentioned discussion showed that the wing-shaped tubes bundle heat exchanger with zero-angle of attack has the best values of h_a, ε and η and hence the best performance comparing with the other bundles.

V. CONCLUSIONS

Heat transfer characteristics and thermal performance criteria of wing-shaped tubes bundle placed in cross-flow have been numerically and experimentally investigated for $1.8 \times 10^3 \leq Re_a \leq 9.7 \times 10^3$. Different tubes arrangements for various $\theta_{1,2,3}$ were considered. $\theta_{1,2,3}$ was changed from 0° to 315° (0°, 45°, 135°, 225°, 315°) experimentally and from 0° to 330° (0°, 30°, 45°, 135°, 150°, 180°, 210°, 225°, 315°, and 330°) numerically at the considered Re_a range. Also, the commercial

World Academy of Science, Engineering and Technology
International Journal of Aerospace and Mechanical Engineering
Vol:7, No:6, 2013

CFD software FLUENT 6.3.26 was utilized to predict the flow field around the wing-shaped tubes bundle. Temperature contours were conducted to investigate the effect of different parameters on the heat transfer characteristics. Comparisons between the experimental and numerical results of the present study and those, previously, obtained for similar available studies showed good agreements. The following conclusions are preferred:

1. The results indicated that Nua increases with increasing Rea. In the contrary, St_a decreases as Re_a increases following an inverse power low form. The highest and lowest values of Nu_a and St_a are occurred at $\theta_{1,2,3} = 45°$, $135°$, $225°$, $315°$ and at $\theta_{1,2,3} = 0°$, $180°$, respectively.

2. Correlations were developed from the experimental results for the bundle of wing-shaped tubes to give the average Nu_a and St_a in terms of Re_a and angle of attack. The general form of the correlations are:

$$Nu_a = a.(Re_a)^b.(Pr)^{1/3}.\left(1 + \frac{\theta°}{\theta_{90°}°}\right)^c$$

$$St_a = a.(Re_a)^{b-1}.(Pr)^{-2/3}.\left(1 + \frac{\theta°}{\theta_{90°}°}\right)^c$$

3. The air flow heat transfer results of the present study were compared with previous correlations reported in literature, which having different tubes shapes, with the same surface area and similar parameters as for the wing-shaped ones. The studied bundle with zero angle of attack has increased values of Nu_a by about 24% and 76% comparing with those obtained for circular and elliptical tubes, respectively. While $\theta_{1,2,3} = 45°$, the values of Nu_a were more than those for the elliptical tubes bundle by about 64 %.

4. The highest values of ha were obtained for arrangement of $\theta_{1,2,3} = 0°$ while the lowest ones were obtained for $\theta_{1,2,3} = 45°$, $135°$ for all values of Re_a at certain ΔP_a. Also, the studied bundle has the higher value of h_a at $\theta_{1,2,3} = 0°$ followed by $180°$, and $30°$, comparing with the circular and elliptical tubes bundles, at the same Re_a and ΔP_a. Conversely, the elliptic tubes bundle has a higher h_a than that of the studied bundle at $\theta_{1,2,3} = 45°$.

5. ε decreased with Re_a increasing and the highest and lowest values of ε were occurred at $Re_a = 1.8 \times 10^3$ and 9.7×10^3, respectively.

6. The highest and lowest values of ε, for all the studied arrangements, were occurred at the lowest and highest values of Re_a, respectively, while the highest and lowest values of ε at every Re_a are occurred at $\theta_{1,2,3} = 0°$, $180°$ and $\theta_{1,2,3} = 45°$, $225°$, respectively.

7. A correlation of ε for various $\theta_{1,2,3}$ at $1.8 \times 10^3 \leq Re_a \leq 9.7 \times 10^3$ was obtained as follows:

$$\varepsilon = a \ (Re_a)^b \ (Pr)^{1/3} \ (1 + \frac{\theta°}{\theta_{90°}})^c$$

8. It is evident that the wing-shaped tubes heat exchanger with zero angle of attack has the highest values of (η) followed by the angles of $30°$ and $45°$. The studied heat exchanger with zero angle of attack has the highest values of η comparing with those of elliptical ones at different flow angles of attack.

9. The wing-shaped tubes bundle heat exchanger with zero-angle of attack has the best values of h_a, ε and η and hence the best performance.

NOMENCLATURE

Alphabet- Upper Case

A_{so}	Total outer surface area of the tubes, m^2
D_{eq}	Equivalent circular diameter, m
Nu	Nusselt number, $(h.D_{eq})/k$
P_{dc}	Pressure drop coefficient, $(2.\Delta P_a)/(\rho_{af}.V_a^2)$
Pr	Prandtl number, $(\mu. c_p)/k$
Q	Heat transfer rate, W
R^2	coefficient of determination ranged from 0 to 1
Re	Reynolds number, $(\rho.V.D_{eq})/\mu$
St	Stanton number, $Nu/(Re_a.Pr)$
T	Temperature, K
V	Velocity, m/s

Alphabet- lower Case

c_p	Specific heat at constant pressure, J/kg.K
h	Heat transfer coefficient, W/m^2.K
k	Thermal conductivity, W/m.K
m	Mass flow rate, kg/s
t	Tube thickness, m
x	Axial coordinate
y	The normal distance to the tube surface
y^+	Dimensionless normal distance to the tube surface

Greek symbols

ε	Effectiveness, $(\rho_{af}.c_{pf}(T_{ai}-T_{ae}))/\Delta P_a$
μ	Absolute viscosity, Pa.s
η	Efficiency Index, $(St/St_c)/(P_{dc}/P_{dcc})$
ρ	Density, kg/m^3
α or θ	Angle of attack, °
Δh_{dyn}	Dynamic head difference, m H$_2$O
ΔP_a	Pressure drop across the bundle, Pa

Subscripts:

a	Air
c	Circular
e	Exit
f	Film
i	Inlet, or row number
o	Outer or outlet
w	Water

Abbreviations

RNG	Reynolds normalized group

REFERENCES

[1] A. Zhukauskas, R. V. Ulinskas, Efficiency parameters of heat transfer in tube banks, Heat Transfer Engineering, Vol.6, No.1, PP.19-25, 1985.
[2] S. A. Nada, H. El-Batsh, M. Moawed, Heat transfer and fluid flow around semi-circular tube in cross flow at different orientations, International Journal of Heat Mass Transfer, Vol. 43, PP. 1157–1169, 2007.

[3] H. Brauer, Compact heat exchangers, J. Chem. Process Eng, pp. 451-460, 1964.

[4] A. Horvat, M. Leskovar, B. Mavko, Comparison of heat transfer conditions in tube bundle cross-flow for different tube shapes, International Journal of Heat and Mass Transfer, Vol. 49, pp. 1027-1038, 2006.

[5] H. Nishiyama, T. Ota, T. Matsuno, Heat transfer and flow around elliptic cylinders in tandem arrangement, JASME Int. J., Ser. II, Vol. 31, No. 3, PP. 410–419, 1988.

[6] D. K. Harris, V. W. Goldschmidt, Measurements of the overall heat transfer from combustion gases confined within elliptical tube heat exchangers, Exp. Thermal Fluid Sci., Vol. 26, PP. 33–37, 2002.

[7] T. A. Ibrahim, A. Gomma, Thermal performance criteria of elliptic tube bundle in cross flow, International Journal of Thermal Sciences, Vol. 48, PP. 2148-2158, 2009.

[8] E. Z. Ibrahiem, A. O. Elsyed, E. S. Sayed Ahmed, Experimental investigation of the performance of a cross flow heat exchanger with bundle of semi-circular tubes, Mansoura Engineering Journal(MEJ), Vol.28, No.2, 2003.

[9] E. Z. Ibrahiem, A. O. Elsyed, E. S. Sayed Ahmed, Experimental study of air cooling and dehumidification around an in-line elliptic tubes bank in cross flow heat exchanger, The International Engineering conference, Mutah, Jordan, 2003.

[10] M. G. Khan, A. Fartaj, D. S-K. Ting, An experimental characterization of cross-flow cooling of air via an in-line elliptical tube array, International Journal of Heat and Fluid Flow, Vol. 25, PP. 636–648, 2004.

[11] N. Mangadoddy, R. Prakash, R. P. Chhabra, R. V. Eswaran, Forced convection in cross flow of power law fluids over a tube bank, Chemical Engineering Science, Vol. 59,PP. 2213 – 2222, 2004.

[12] E. Ibrahim, M. Moawed, Forced convection and entropy generation from elliptic tubes with longitudinal fins, Energy Conversion and Management, Vol. 50, PP. 1946 – 1954, 2009.

[13] E. S. Sayed Ahmed, O. M. Mesalhy, T. M. Khass, and A. H. Hassan, Parametric study of air cooling process via water cooled bundle of wing-shaped tubes, EIJST, Vol. 15, No. 3, Sept. 2012.

[14] Y. A. Cengel, Heat transfer a practical approach, McGraw- Hill, New Jersey, 1998.

[15] FLUENT 6.3.26 User's Guide, FLUENT Inc, 2006.

[16] A. Zukauskas, Heat transfer from tubes in cross flow in Advances in Heat Transfer, Edited by Hartnett, J. P. and Irvine, T. F. Jr, New York: Academic Press. Vol. 8, pp. 93-160, 1972.

[17] A. Bergles, A. Blumenkra, J. Taborek, Performance evaluation criteria for enhanced heat transfer surfaces, 4th Int. Heat Transfer Conference, Vol. 2, PP. 239–243, 1974.

[18] A. Gomaa, R. LeFeuvre, C. Underwood, T. Bond, Numerical analysis of developing laminar flow and heat transfer characteristics through corrugated wall channels, IMechE 6th UK National Conference on Heat Transfer, UK, pp. 205–214, 1999.

[19] R. Afify, N. Berbish, A. Gomaa, A. Eid, Numerical and experimental study of turbulent flow and convective heat transfer in a circular tube with disc-baffles, Engineering Research Journal 96, M37–M61, Faculty of Eng. at Mattaria, Egypt, 2004.